electronics

Article

A Negative Emotion Recognition System with Internet of Things-Based Multimodal Biosignal Data

Seung-Mi Ham [1], Hye-Min Lee [1], Jae-Hyun Lim [2] and Jeongwook Seo [1,*]

[1] School of Computing and Artificial Intelligence, Hanshin University, Osan 18101, Republic of Korea; djs2ys@hs.ac.kr (S.-M.H.); alsl0903@hs.ac.kr (H.-M.L.)
[2] Platform Development Team, Wright Brothers Co., Ltd., Seoul 04384, Republic of Korea; windsor@wrightbrothers.kr
* Correspondence: jwseo@hs.ac.kr

Abstract: Previous studies to recognize negative emotions for mental healthcare have used heavy equipment directly attaching electroencephalogram (EEG) electrodes to the head, and they have proposed binary classification methods to identify negative emotions. To tackle this problem, we propose a negative emotion recognition system to collect multimodal biosignal data such as five EEG signals from an EEG headset and heart rate, galvanic skin response, and skin temperature from a smart band for classifying multiple negative emotions. This consists of an Android Internet of Things (IoT) application, a oneM2M-compliant IoT server, and a machine learning server. The Android IoT application uploads the biosignal data to the IoT server. By using the biosignal data stored in the IoT server, the machine learning server recognizes the negative emotions of disgust, fear, and sadness using a multiclass support vector machine (SVM) model with a radial basis function kernel. The experimental results demonstrate that the multimodal biosignal data approach achieves 93% accuracy. Moreover, when considering only data from the smart band, the system achieved 98% accuracy by optimizing the hyperparameters of the multiclass SVM model. Based on these results, we plan to develop a metaverse system that detects and expresses negative emotions in real time.

Keywords: emotion recognition; multimodal; biosignal; wearable device; Internet of Things; support vector machine

Citation: Ham, S.-M.; Lee, H.-M.; Lim, J.-H.; Seo, J. A Negative Emotion Recognition System with Internet of Things-Based Multimodal Biosignal Data. *Electronics* **2023**, *12*, 4321. https://doi.org/10.3390/electronics12204321

Academic Editors: George A. Papakostas and Simeone Marino

Received: 1 September 2023
Revised: 1 October 2023
Accepted: 15 October 2023
Published: 18 October 2023

1. Introduction

As information technology (IT) develops and the interest in personal health increases, the demand for wearable devices such as smart bands and smartwatches is increasing [1,2]. These devices enable the collection of various biosignal data, and the collected biosignal data are applied in various fields, such as health monitoring, medical care, and emotion recognition [3,4]. In addition, with the popularization of user-customized intelligent services and the development of artificial intelligence technology, research on emotion recognition using biosignal data is becoming more important [5–7]. Previous research on emotion recognition was based on voice recognition, facial expression recognition, and gesture recognition. However, these studies often face challenges in accurately identifying actual emotional states because individuals may intentionally hide or distort their true feelings [8]. On the other hand, biosignals cannot be intentionally manipulated since they change without one's awareness [9]. Furthermore, biosignals can objectively recognize not only superficial emotions but also inner emotional states. For this reason, emotional recognition studies using biosignal data have been attracting attention. Emotion recognition studies usually focus on classifying six basic types of emotions: happiness, sadness, anger, disgust, fear, and surprise [10]. However, to manage the negative emotions that may harm our mental health, it is necessary to focus on the negative emotions (e.g., disgust, fear, and sadness). Previous studies for recognizing negative emotions have mainly used a unimodal approach using only a single type of sensor to determine negative emotions. In particular, they typically attached electroencephalogram (EEG) electrodes directly to the head or used complex heavy equipment systems [11–13]. The equipment used is difficult and complex for ordinary people to wear and has limitations in everyday use. If they use a multimodal approach that effectively utilizes different types of sensor data instead of a unimodal approach, the accuracy of the emotion recognition model can be further improved [14]. In another study, a binary classification method was proposed to determine the predominance of a negative emotion [15]. We propose a negative emotion recognition system that can classify multiple negative emotions, such as disgust, fear, and sadness [16–18]. The multimodal biosignal data are collected through two easy-to-use wearable Internet of Things (IoT) devices. Our aim is to enhance the classification accuracy of various negative emotions (i.e., disgust, fear, and sadness) and make them more accessible to users in their daily lives. The system utilizes an EEG headset to collect five EEG signals (i.e., alpha, beta, gamma, delta, and theta waves). A smart band is used to collect the heart rate (HR), galvanic skin response (GSR), and skin temperature (SKT) data. The multimodal biosignal data are continuously and conveniently collected. We build a multiclass support vector machine (SVM) model with a radial basis function kernel (RBF) by labeling emotions on the collected multimodal biosignal data. We build two different SVM models, one using data from all wearable devices and the other only using the data from the smart band. The purpose is to examine whether good performance can be achieved by using partial data. We compare the results of the two models to determine which approach works better. In addition, we create an optimal model by finding the values of the parameters C and γ that are most suitable for the model.

2. The Proposed Negative Emotion Recognition System

Figure 1 shows the proposed negative emotion recognition system with IoT-based multimodal biosignal data that can be used to manage negative emotions in daily life.

Our proposed system consists of an Android IoT application (APP), a oneM2M-compliant IoT server, and a machine learning server. We will briefly explain the flow of the system. The Android IoT application collects biosignal data and uploads them to the IoT server. The machine learning server receives biosignal data stored in the IoT server using the subscription and notification functions provided by oneM2M and recognizes negative emotions such as disgust, fear, and sadness.

First, we use two easy-to-use wearable IoT devices, an EEG headset and a smart band, to collect multimodal biosignal data. The EEG headset is worn on the head to measure brainwave activity patterns, such as the alpha, beta, gamma, delta, and theta waves. To take measurements, simply place the electrode sensor on the skin of the forehead and attach the ear clip to the earlobe. The smart band is worn on the wrist and measures biosignals such as HR, GSR, and SKT through sensors built into the band. The two wearable IoT devices transmit the multimodal biosignal data to the Android IoT APP installed on the smartphone through Bluetooth. The Android IoT APP checks the received multimodal biosignal data for any changes and then saves the data in the SQLite database. The synchronization service retrieves multimodal biosignal data from the SQLite database once every second and transmits it to the thing adaptation software (TAS) [19]. The TAS transmits the received biosignal data to an IoT client APP using a client socket.

The IoT client APP, modeled as a application dedicated node application entity (ADN-AE), sends a request to the IoT server middleware (MW), modeled as an infrastructure node common service entity (IN-CSE), to register itself [20]. Here, the application dedicated node (ADN) is a node that contains at least one application entity (AE) and does not contain a common service entity (CSE), and the AE is an entity in the application layer that implements application service logic for end-to-end IoT solutions. In addition, the infrastructure node (IN) is a node that contains one CSE and can also contain AEs. The CSE is an entity implemented with 12 common service functions (CSFs) that can be used in common in various application entities of IoT. The 12 CSFs include registration, discovery, security, group management, subscription and notification, etc. [21,22]. When the IoT client

APP receives a response that the ADN-AE has been successfully registered, it requests the IoT server MW to create a container for the EEG headset and a container for the smart band. The IoT server MW creates the two containers in the ADN-AE and sends a response back to the IoT client APP to indicate that the creation is complete. The IoT client APP creates and sends a content instance containing five EEG signals and a content instance containing HR, GSR, and SKT to the IoT server MW. The IoT server MW checks the content instances sent by the IoT client APP and stacks the five EEG signals in the EEG headset container and the HR, GSR, and SKT in the container for the smart band.

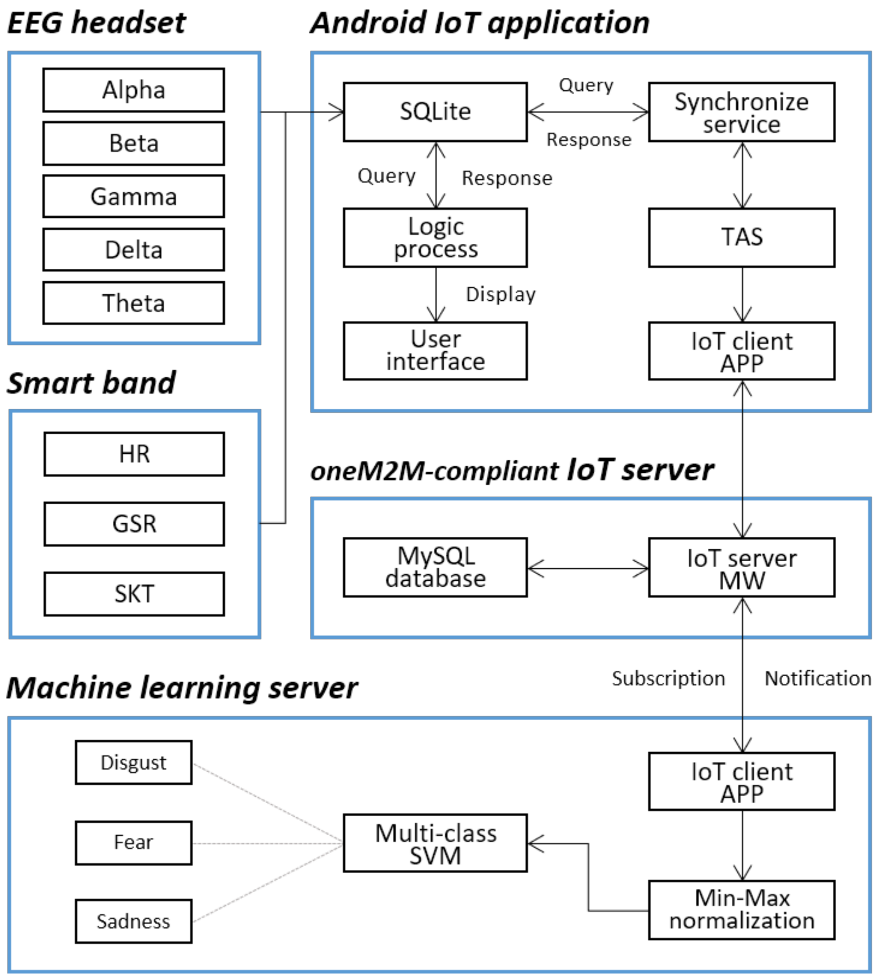

Figure 1. A negative emotion recognition system with IoT-based multimodal biosignal data.

The IoT client APP in the machine learning server subscribes to the resources of the IoT server MW. When a new content instance is uploaded to the IoT server MW, the IoT client APP receives the notification message sent by the IoT server MW and extracts the notification message to obtain the multimodal biosignal data. After that, it normalizes the multimodal biosignal data through a min-max scaler and feeds the normalized data into our multiclass SVM model with a nonlinear RBF kernel to classify the negative emotions such as disgust, fear, and sadness.

3. Exploratory Data Analysis and Multiclass SVM Model

3.1. Exploratory Data Analysis

We collected the multimodal biosignal data from 30 participants for seven emotions: happiness, amusement, disgust, neutral, fear, tenderness, and sadness. As mentioned before, we specifically chose disgust, fear, and sadness as labels that represent negative emotions. Then, we focused on analyzing multimodal biosignal data corresponding to the three negative emotions. We used exploratory data analysis techniques to identify the characteristics, patterns, and structural relationships of the collected multimodal biosignal data.

Figure 2 shows the histograms of the multimodal biosignal data associated with the three negative emotions. The histogram enables the observation of data distribution within specific intervals, facilitating the identification of sections with higher frequencies. In addition, this allows the estimation of the mean, median, and central tendency and the detection of any asymmetries and outliers. The analysis results show that the five EEG signals mainly display a symmetrical distribution and have a single peak. On the other hand, HR, GSR, and SKT data show an asymmetric distribution and have two or more peaks. In particular, the graphs of HR and GSR display a right-skewed shape with the peak on the left and the tail extending to the right.

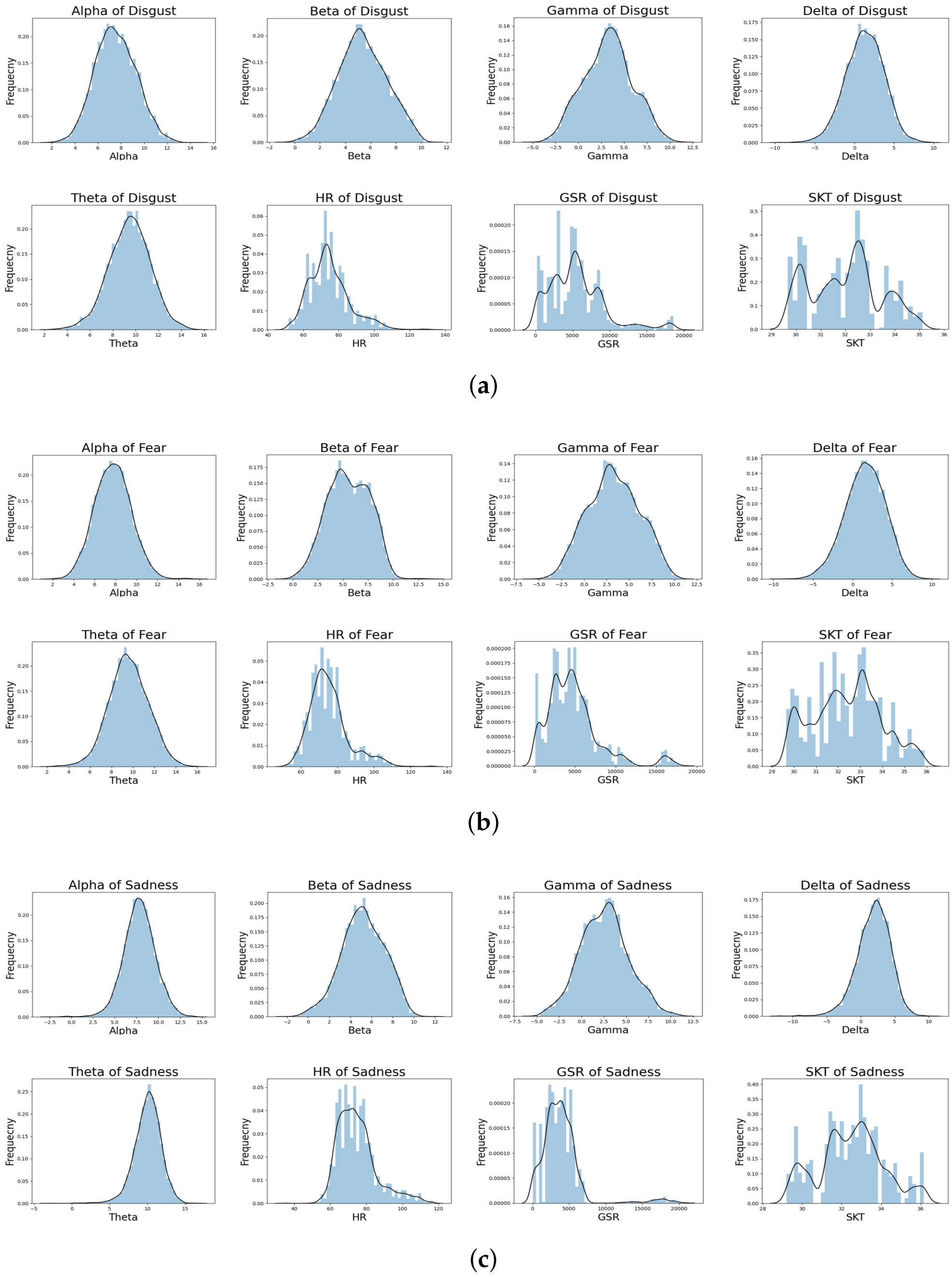

Figure 2. Histograms of the multimodal biosignal data measured from an EEG headset and a smart band for the three negative emotions: (**a**) disgust, (**b**) fear, and (**c**) sadness.

We calculate the covariance between two variables to see how they change together. The covariance has the problem of being affected by the units of the variables. However, the correlation coefficient is not affected by the units of the variables because it non-dimensionally expresses the linear relationship between two variables. In statistics, there are various methods to obtain correlation results between two variables, such as Kendall, Pearson, Spearman, etc. Kendall's Tau is used to measure correlation while preserving the order of data. The Pearson correlation coefficient excels in measuring linear relationships between variables. Spearman correlation is suitable for ranked data. Since we expected the given data to exhibit a linear relationship between variables, we determined that the Pearson correlation coefficient was the most suitable for our research objectives. In Figures 3–5, the Pearson correlation coefficient is used to characterize the degree of linear correlation between two variables [23]. The Pearson correlation coefficient between two variables (x, y) is the quotient of the covariance and standard deviation between the two variables, which is defined as:

$$r(x,y) = \frac{\sum_{n=1}^{N}(x_n - \overline{x})(y_n - \overline{y})}{\sqrt{\sum_{n=1}^{N}(x_n - \overline{x})^2 \sum_{n=1}^{N}(y_n - \overline{y})^2}} \tag{1}$$

where N is the number of samples, and x and y represent the series to be analyzed. $\overline{x}$ and $\overline{y}$ represent the mean value of the observed series. The resulting value of $r(x, y)$ ranges from -1 to 1. A value of 1 indicates a positive correlation where all data points fall well on a straight line and increase as the value increases. A value of -1 means all data points fall on a straight line and a negative correlation decreases as the coefficient increases. A value of 0 means that there is no linear relationship between the two variables [24,25].

The correlation matrices made from the Pearson correlation coefficient show that the larger the absolute value of the coefficient, the narrower the ellipse, and the smaller the absolute value, the wider the ellipse appears. Next, we summarize the analysis result in each negative emotion state. In the disgust state, the beta and gamma waves showed positive values of 25% and 20%, respectively. These findings suggest a strong positive correlation between beta and gamma waves in the state of disgust. In the fear state, beta waves, gamma waves, and HR showed positive values of 20%, 15%, and 21%, respectively. This indicates a significant positive correlation between the fear state and beta waves, gamma waves, and HR. Finally, in the sadness state, beta waves, gamma waves, and SKT showed positive values of 10%, 15%, and 10%, respectively. These results suggest a strong positive correlation between the state of sadness and beta waves, gamma waves, and SKT.

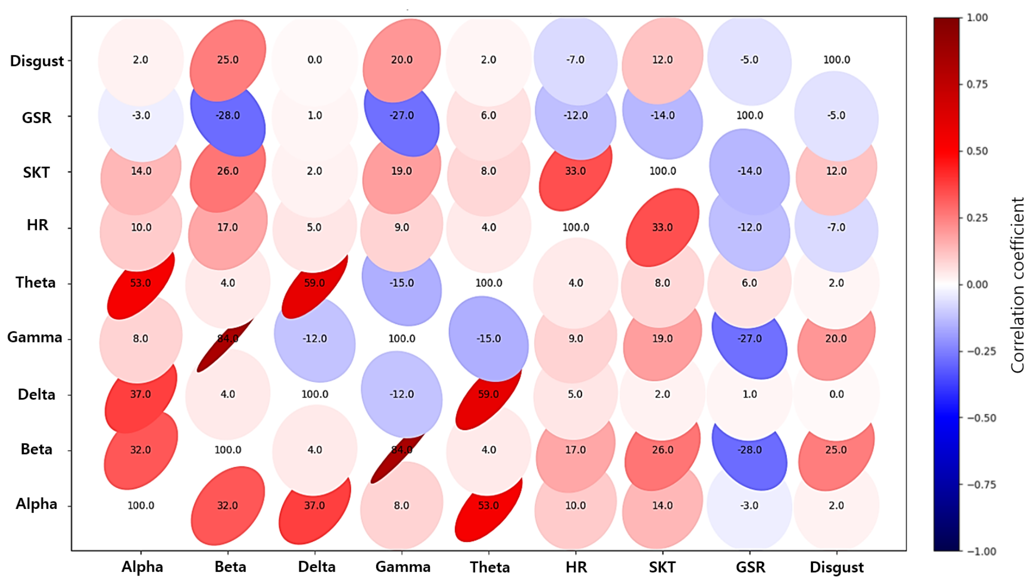

Figure 3. Correlation matrix of multimodal biosignal data for the disgust state.

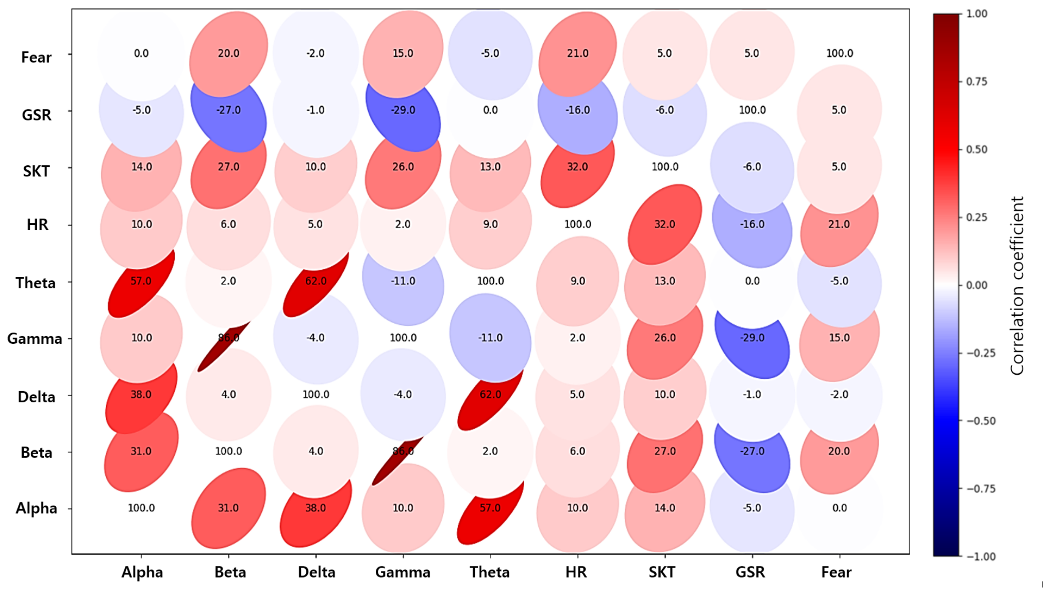

Figure 4. Correlation matrix of multimodal biosignal data for the fear state.

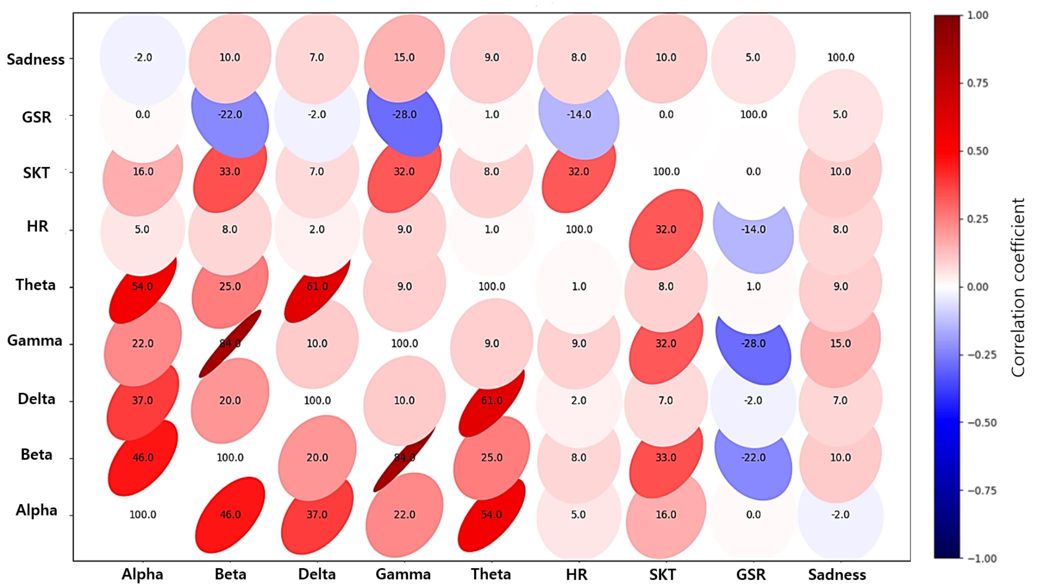

Figure 5. Correlation matrix of multimodal biosignal data for the sadness state.

3.2. Multiclass Nonlinear SVM Model

Machine learning models such as decision trees, random forests, k-nearest neighbors (KNNs), artificial neural networks (ANNs), and SVMs are frequently used to classify data. The decision tree is inflexible in parametric modeling; random forest is limited to handling high-dimensional datasets; and KNN is quite slow and very sensitive to outliers when dealing with large amounts of data. ANN makes their internal parameters difficult to adjust, which can lead to underfitting and overfitting problems [26]. On the other hand, SVM has a high classification accuracy and a good ability to handle high-dimensional and large datasets [27]. Therefore, it is widely used in the field of classification and is suitable for classifying linear and nonlinear data. It also achieves high accuracy using kernel functions that map the data into higher dimensions, improving the classification of nonlinear data [28]. In this study, considering the need for a technique specialized in handling nonlinear elements, we chose a nonlinear SVM model. Specifically, we chose the RBF kernel, known for its effectiveness in handling datasets with nonlinear data distributions. The RBF kernel facilitates the linear separation in high-dimensional spaces by virtue of nonlinear feature mapping and proves highly valuable when confronted with diverse types of data. Consequently, we propose a multiclass SVM with the RBF kernel. The multimodal biosignal dataset for training the proposed model is partitioned into an 80% training set and a 20% test set. We normalize all features of the training and test data by scaling them within ranges [0, 1] through a Min-Max scaler to make it more suitable for training. A multimodal biosignal dataset labeled with a training pattern can be represented by

$$D_N = \{(\boldsymbol{x}_1, y_1), \cdots, (\boldsymbol{x}_N, y_N)\} = \{(\boldsymbol{x}_n, y_n)\}_{n=1}^{N} \tag{2}$$

where $\boldsymbol{x}_n = [x_{1,n}, x_{2,n}, \cdots, x_{K,n}]^T$ denotes a training feature vector of length K, and $y_n \in \{1, 2, \cdots, M\}$ denotes a label among M classes. The SVM model finds the marginally separated hyperplane that maximally represents the distance from each class's hyperplane to the nearest feature vector, called the support vector. It utilizes a kernel function to map data from a low-dimensional space to a high-dimensional space to create a nonlinearly separable pattern. A multiclass SVM model built using an RBF kernel is represented by Equation (3). It splits a multiclass dataset into multiple binary classification problems and uses a one-versus-rest method which is a heuristic method using binary classifiers.

$$\hat{y}_{\text{new}} = \underset{m=1,2,\cdots,M}{\text{argmax}} \sum_{n \in S} \alpha_{m,n} y_{m,n} L(\boldsymbol{x}_n, \boldsymbol{x}_{new}) + b_m \tag{3}$$

where S denotes the set of support vectors, and $\alpha_{m,n}$ represents the Lagrange multiplier with the constraint $0 \le \alpha_{m,n} \le C$ on class m. C denotes the hyperparameter that determines the trade-off for margin and error, $y_{m,n}$ represents the temporary label, and b_m denotes the bias term. In addition, the RBF kernel is represented by Equation (4).

$$L(\boldsymbol{x}_n, \boldsymbol{x}_{new}) = exp(-\delta \|\boldsymbol{x}_n - \boldsymbol{x}_{new}\|_2^2) \tag{4}$$

where δ denotes a hyperparameter that defines the extent to which the influence of the training vector $\boldsymbol{x}_n$ reaches the support vectors, and $\|\cdot\|_2$ denotes the L2 norm [29]. The smaller the value of δ, the greater the effect of x_n on the classification of x, resulting in a larger variance. The larger the value of δ, the smaller the effect of x_n on the classification of x, resulting in a smaller variance.

4. Experimental Results

4.1. Experimental Conditions

We used an EEG headset and a smart band, which are commercially available devices to develop Android IoT applications, for collecting various biosignal data such as alpha waves, beta waves, gamma waves, delta waves, theta waves, HR, GSR, and SKT. To construct the training dataset for building the multiclass SVM model, we exploited pre-labeled video clips in [30] displaying one of seven emotion categories covering common emotional contexts: anger, sadness, fear, disgust, amusement, tenderness, and neutral. Although the video clips, as mentioned in [30], were carefully selected to meet various criteria, and their validity was confirmed through multidimensional evaluation experiments, we conducted an experimental survey to make a more objective and comprehensive training dataset. Participants were shown these video clips and their biosignal data were collected. Simultaneously, they provided an emotional evaluation of the video clips through the survey. We then extracted biosignal data corresponding to video clips that received an emotional score of 3 or higher, which formed our training dataset. By integrating both biosignal data and emotional ratings, we captured not only the physiological responses of participants (through biosignal data) but also their subjective emotional experiences (through emotional ratings). Furthermore, we ensured the reliability and consistency of emotional ratings by only including data related to video clips that received a score of 3 or higher.

Figure 6 illustrates the experimental components of the proposed emotion recognition system. The experimental components are used for collecting multimodal biosignals in various emotions. The system includes two wearable IoT devices (i.e., an EEG headset and a smart band), an android IoT APP, a oneM2M-compliant IoT server, and movie clips encapsulating different emotions. Figure 7 shows the experimental setup to collect multimodal biosignal data from subjects watching the movie clips. A total of 30 healthy young adults participated as test subjects in the experiment, comprising 23 males and 7 females, with a mean age of 23.2 ± 2.1 years (20–27 years old). Although sex imbalances exist in our study, we found in [30] that differences in subjective arousal levels and negative affect between women and men did not reach statistical significance. We scaled all video clips that the subjects would be watching to the same resolution (1920 × 1080 pixels) and displayed them on a 24-inch liquid crystal display (LCD) screen. In addition, two loudspeakers were placed, and the volume was adjusted to an appropriate level so that the subjects could watch the movie comfortably [31]. The subjects wore the EEG headset on their heads and the smart band on their wrists. The movie clips were played at random, and we avoided the continuous playback of movie clips displaying similar emotions. While watching the video, the subjects were asked to fill out a questionnaire for the survey in Figure 8 used to self-record the subject's emotional state while watching the movie clips.

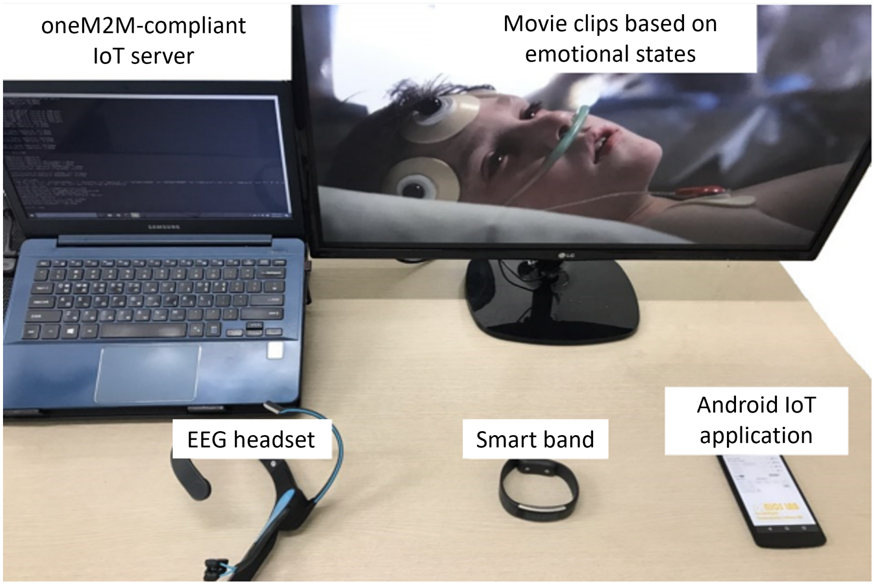

Figure 6. Experimental components for multimodal biosignals collection in various emotions.

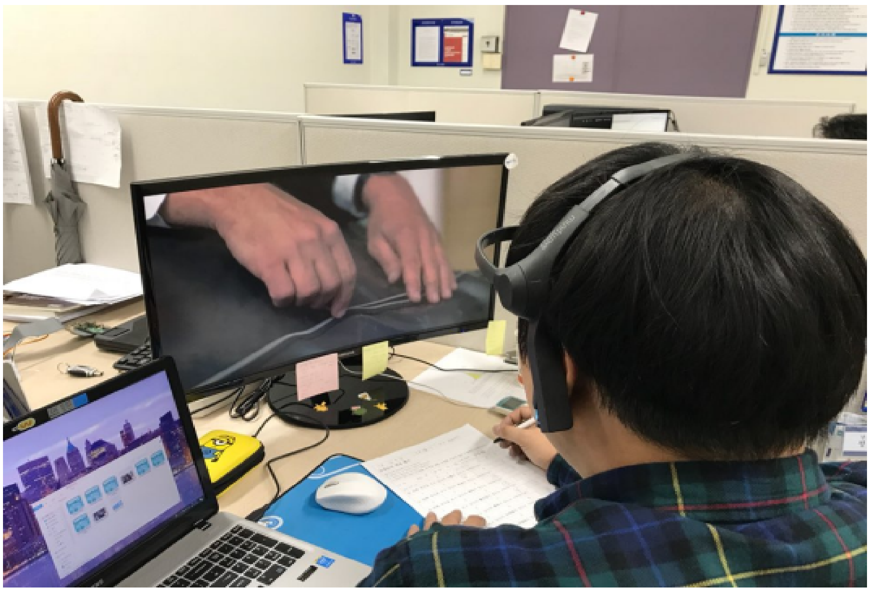

Figure 7. Experimental process for collecting multimodal biosignals through watching movie clips.

Name :		Sex : male( ) female( )		Student ID :
Emotion recognition video evaluation				
Thank you for participating in the survey. This survey evaluates your emotions after watching each video. This data will only be used for the research of the paper. Please indicate your satisfaction with each question. (1 = low, 2 = slightly low, 3 = normal, 4 = slightly high, 5 = high)				
Age :			Family background :	
Video start time :			Video end time :	
How angry were you when you saw the first video?				
1	2	3	4	5
How sad were you when you saw the second video?				
1	2	3	4	5
How fearful were you when you saw the third video?				
1	2	3	4	5
How disgusted were you when you saw the fourth video?				
1	2	3	4	5
How amused were you when you saw the fifth video?				
1	2	3	4	5
How tender did you feel when you saw the sixth video?				
1	2	3	4	5
How neutral did you feel when you saw the seventh video?				
1	2	3	4	5

Figure 8. The questionnaire to record emotional responses while watching the videos.

4.2. Performance Evaluation

Figure 9 shows the experimental results for the linear SVM model, the nonlinear SVM model with an RBF kernel (default), and the nonlinear SVM using an RBF kernel with specific parameters ($C = 10$, $\gamma = 10$). In Figure 9, F1–F8 are cases in which all multimodal biosignal data (i.e., five EEG signals, HR, GSR, and SKT) collected from the two wearable IoT devices are used. F6–F8 are cases in which only the HR, GSR, and SKT data collected from the smart band are used. Through this, we compared the average accuracy of the linear SVM model and the nonlinear multiclass SVM and confirmed that the multiclass SVM model achieved higher accuracy. Comparing the results from the linear SVM model and the multiclass SVM (default) using the RBF kernel, F1–F8 are more accurate than F6–F8, but the difference in accuracy is about 2.7–2.8, which is relatively small. This suggests that building a model with only HR, GSR, and SKT collected from a smart band may be more efficient than using all of the multimodal biosignal data collected from two wearable IoT devices. A comparison of the multiclass SVM using an RBF kernel (default) and the multiclass SVM using an RBF kernel ($C = 10$, $\gamma = 10$) shows that the parameter values have a significant effect on accuracy. Therefore, higher accuracy can be achieved by selecting appropriate parameter values and incorporating them into the model.

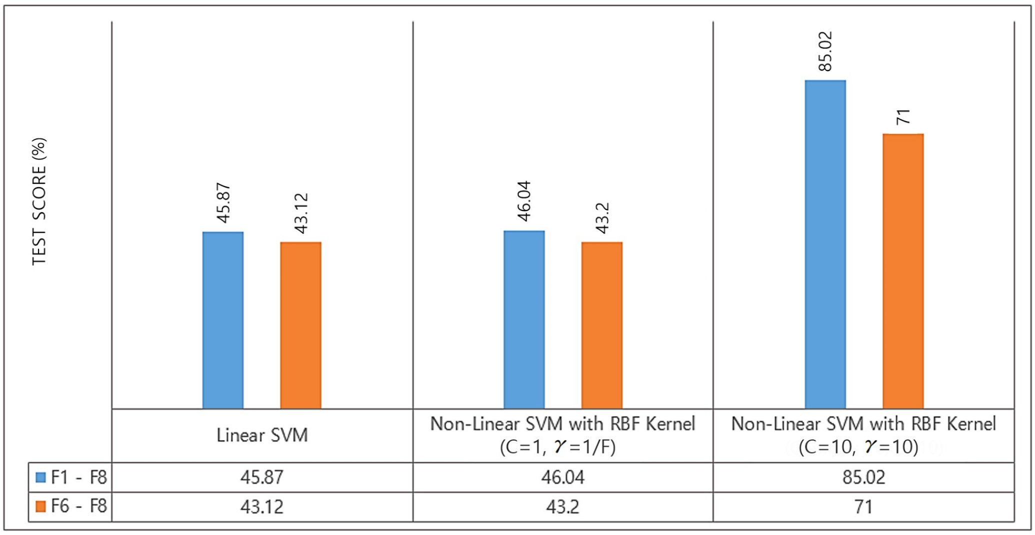

Figure 9. Average accuracy comparison according to the SVM model.

A grid search was performed to determine the optimal parameter values for the model, and the accuracy according to parameter adjustment is shown as heatmaps in Figures 10 and 11. When performing a grid search, the parameter values for C and γ ranged from 10^{-3} to 10^{3}. Figure 10 shows a heatmap representing the accuracy for different parameter values of the multiclass SVM (with an RBF kernel) consisting of multimodal biosignal data (five EEG signals, HR, GSR, and SKT). The highest accuracy of 93% was achieved with parameter values of $C = 10$, 10^2, 10^3, and $\gamma = 10^2$. Cross-validation confirmed that the most appropriate model was obtained when $C = 10$ and $\gamma = 10^3$. Figure 11 displays a heatmap showing the accuracy according to the parameter values of the multiclass SVM (with an RBF kernel) consisting of HR, GSR, and SKT. It is shown that the highest accuracy of 98% was achieved when the parameter values are $C = 10$, 10^2, 10^3, and $\gamma = 10^3$. Moreover, cross-validation has shown that the optimal model was obtained when $C = 10^3$ and $\gamma = 10^3$. Therefore, this demonstrates that, by adjusting the parameter values, the model consisting of HR, GSR, and SKT collected from a smart band can achieve a higher accuracy than the model consisting of multimodal biosignal data collected from two wearable IoT devices.

Table 1 shows the performance of a multiclass SVM (with an RBF kernel) consisting of HR, GSR, and SKT from the smart band. The evaluation indicators used for the performance comparison are introduced and defined as shown in Table 2. Following the definitions from Table 2, the three widely used metrics of precision, recall, and F1 score can be calculated as follows:

$$Precision = \frac{TP}{TP + FP} \tag{5}$$

$$Recall = \frac{TP}{TP + FN} \tag{6}$$

$$F1 = \frac{2(Precision * Recall)}{Precision + Recall} \tag{7}$$

Precision refers to the model's ability to distinguish between negative emotions. Higher precision values improve the model's ability to distinguish between similar negative emotions. Recall reflects the proportion of models capable of solving the intraclass similarity problem. A higher recall value improves the model's ability to detect negative emotions with intra-class similarity. The F1 score represents the balance between precision and recall. The higher the F1 score, the more powerful the model performance.

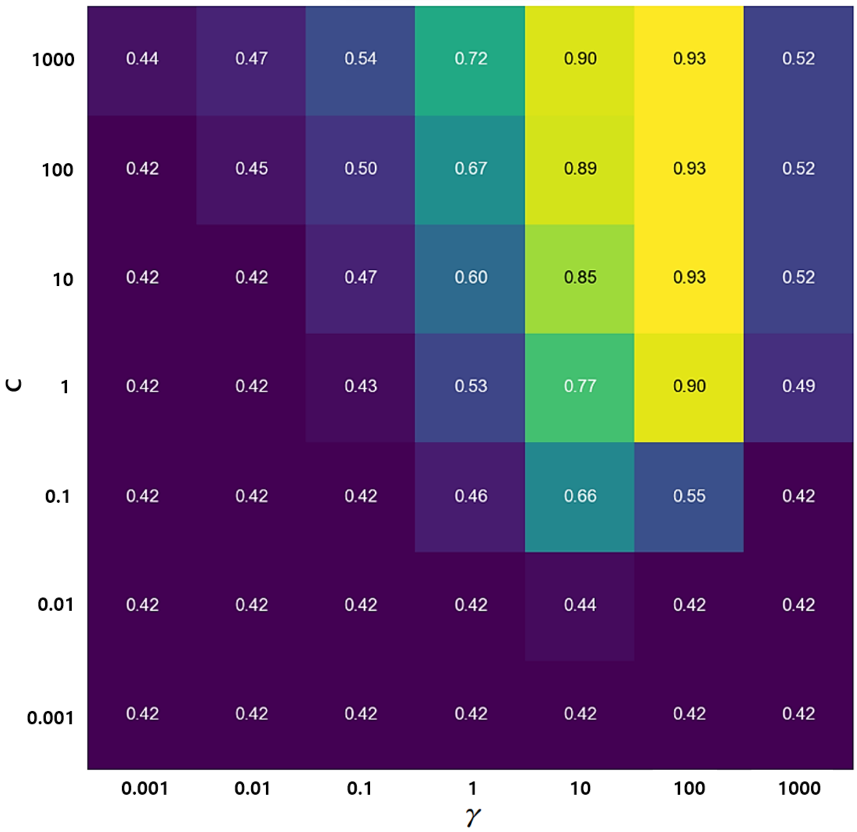

Figure 10. Heatmap according to the multimodal biosignal data of the two wearable IoT devices.

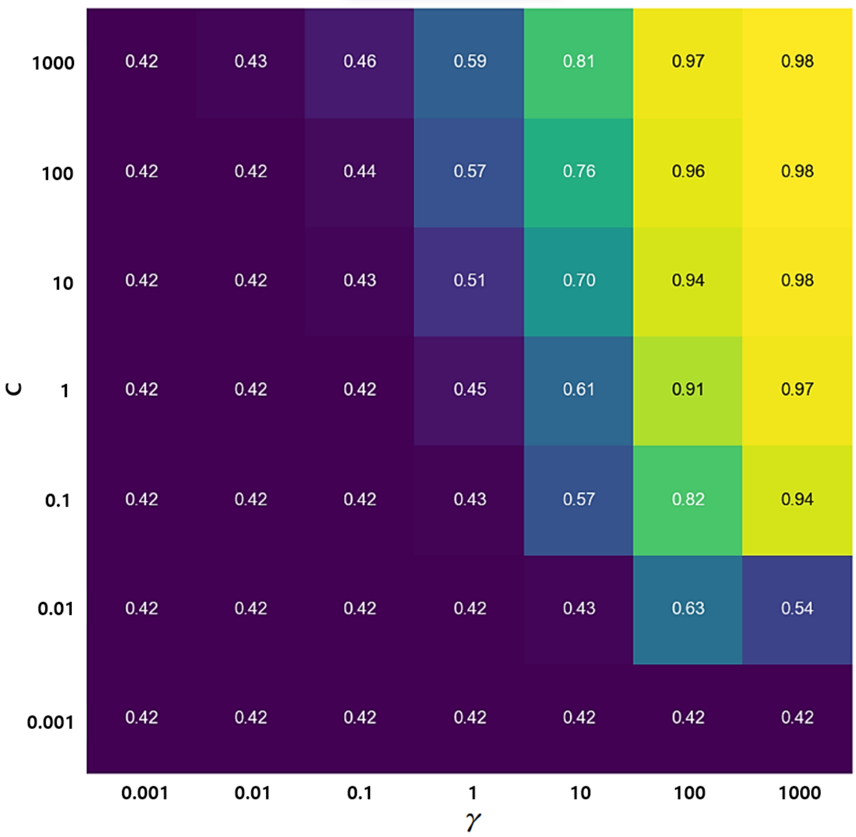

Figure 11. Heatmap according to the biosignal data of the smart band.

Table 1. Performance of multiclass SVM consisting of HR, GSR, and SKT.

	Precision	Recall	F1 Score	Support
Disgust	0.97	0.97	0.97	1504
Fear	0.98	0.98	0.98	2395
Sadness	0.99	0.99	0.99	1707
Accuracy			0.98	5606
Macro average	0.98	0.98	0.98	5606
Weighted average	0.98	0.98	0.98	5606

Table 2. Definition of terms for evaluation indicators.

True positive (TP)	A target traffic sign has been predicted to a correct type.
True negative (TN)	A non-target traffic sign has been predicted to a correct type.
False positive (FP)	A target traffic sign has been predicted to a wrong type.
False negative (FN)	A non-target traffic sign has been predicted to a wrong type.
Macro-average	Averaging the unweighted mean per label.
Weighted average	Averaging the support-weighted mean per label.

Figure 12 illustrates the learning curve of a multiclass SVM model ($C = 10^3$, $\gamma = 10^3$) constructed using HR, GSR, and SKT data from the smart band. The model's score is expressed as a percentage and shows how accuracy changes as the amount of training data increases. It presents the model's performance on both the training and cross-validation sets. In the graph, the training score decreases from 99.8% to 99.2%, and the cross-validation score increases from 92.7% to 98.1%. These results indicate that both the training curve and cross-validation curve of the model perform well, confirming the absence of the overfitting problem. In addition, we verified the appropriateness of the parameter values C and γ selected for the model.

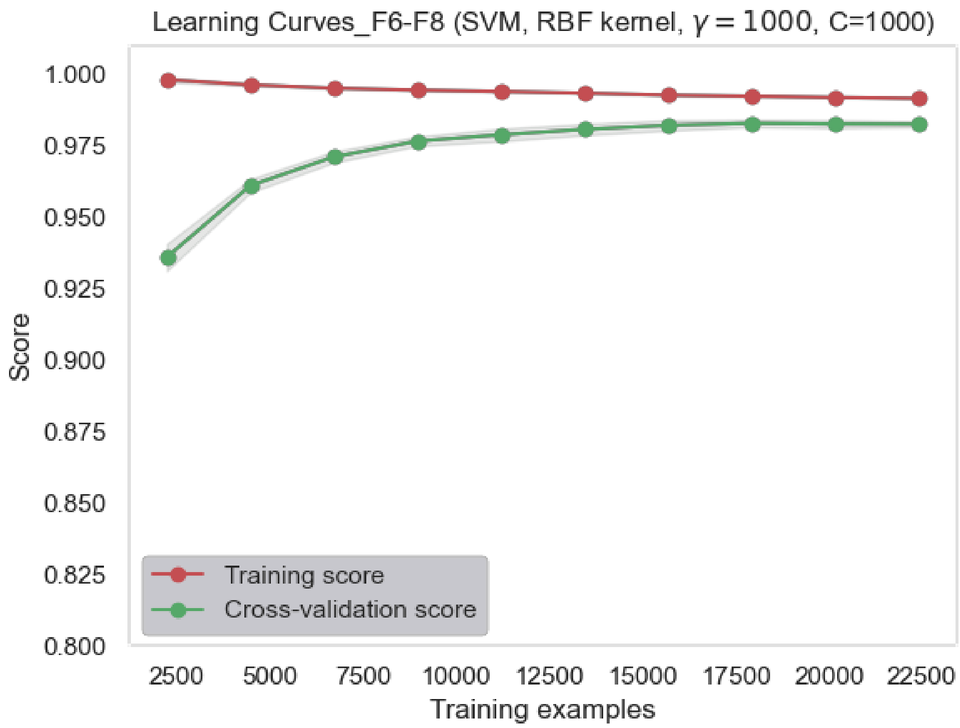

Figure 12. The learning curve for the multiclass SVM model built using HR, GSR, and SKT.

5. Discussion

We compare our study with studies that have investigated negative emotion recognition using biosignal data, similarly to our approach. Table 3 summarizes the comparison. Key observations are summarized below.

Table 3. Comparisons between our work and existing works.

Study	Year	Emotion	Biosignal	Data Collection Tool	Method
Ihmig et al. [32]	2020	Anxiety	ECG, GSR, RSP	Biofeedback system, BITalino biosignal measurement device, Ag/AgCl electrodes	Bagged trees
Lee and Yoo [12]	2020	Negative	ECG, GSR, SKT	MP 150TM of BIOPAC	LSTM
Al-Jumaily et al. [33]	2021	Stress	ECG, EMG	Certain sensors	Gaussian kernel SVM
Mekruksavanich et al. [34]	2022	Tension	ECG, EMG, GSR	Chest-worn equipment	CNN, ResNeXt
Our study	2023	Disgust, fear, sadness	HR, GSR, SKT	Microsoft Band 2	RBF kernel SVM

In [32], a study aiming to classify anxiety levels into two and three categories was conducted by utilizing a combination of features extracted from ECG (electrocardiogram), GSR, and RSP (respiration) signals. A biofeedback system, the BITalino biosignal measurement device, and Ag/AgCl electrode were used to collect biosignal data, and a bagged tree was used as the model learning method. In [12], a model that recognizes neutral and negative emotions by utilizing the biosignals of ECG, GSR, and SKT was proposed. The biosignal data were collected using the MP 150TM from BIOPAC Systems, and the emotion recognition model was designed by applying long short-term memory (LSTM). A Gaussian kernel SVM model to detect stress states was proposed in [33]. The biosignal data were collected using specific sensors that measure ECG and electromyogram (EMG) and classified stress states accordingly. In [34], a framework to classify tension using biosignal data (ECG, EMG, GSR) from chest-worn equipment was proposed. A convolutional neural network (CNN) based on ResNeXt was presented [35].

Existing studies mainly adopt data collection tools that require users to wear heavy equipment, but this method has several limitations. First, these devices are large and heavy, which can cause discomfort to the user. Also, it is difficult to wear these devices for long periods of time, which limits movement and can limit data collection in real-world environments. Lastly, if users are required to attach certain sensors themselves, they must understand exactly how to use the equipment, which can be difficult for some users. In our proposed system, we considered user convenience and used the Microsoft Band 2 smart band. This smart band is easy to wear, and we can conveniently collect HR, GSR, and SKT data. Furthermore, while previous studies classified negative emotions into stages or binary categories, our study classifies negative emotions more specifically into disgust, fear, and sadness, providing a more detailed classification of negative emotions.

6. Conclusions

Existing research on recognizing negative emotions faces challenges related to everyday user accessibility and is limited to simplistic binary classification. In this paper, a negative emotion recognition system that can classify multiple negative emotions (i.e., disgust, fear, and sadness) is proposed. The system is based on an IoT server that continuously collects multimodal biosignal data from two wearable IoT devices: an EEG headset and a smart band. The data collected is stored in real-time within the database of the oneM2M-based IoT server MW. In addition, we built a multiclass SVM with an RBF kernel that can more accurately classify the negative emotions. An accuracy comparison between linear and nonlinear SVM models showed that the nonlinear SVM models with an RBF kernel achieve higher accuracy. Two different datasets were used to evaluate the performance of the SVM models: one consisting of multimodal biosignal data collected from the two wearable IoT devices and the other consisting of HR, GSR, and SKT data collected from the smart band. The accuracy of the model trained with multimodal biosignal data was only slightly better than that of the model trained with HR, GSR, and SKT data, essentially showing no significant difference in accuracy. This observation led to the conclusion that we can improve the efficiency of the model by only utilizing HR, GSR, and SKT. Using grid search, we found the optimal parameter values $C = 10^3$ and $\gamma = 10^3$ for the model. The multiclass SVM model built using only HR, GSR, and SKT with optimal parameters achieved an average accuracy of 98%. This is 5% higher than the accuracy achieved by the model constructed using the multimodal biosignal data from both wearable IoT devices. Future research will focus on achieving a higher emotion detection accuracy using only the biosignal data from a smart band. Our goal is to develop a system that accurately detects the negative emotions of users wearing smart bands in real-time. We also plan to project these emotions in real-time to digital humans within the metaverse. Since our research is currently limited to negative emotions, we plan to expand our research to recognize a broader range of emotions and more subtle emotional states.

Author Contributions: Methodology, J.-H.L.; Investigation, H.-M.L.; Writing—original draft, S.-M.H.; Supervision, J.S. All authors have read and agreed to the published version of the manuscript.

Funding: This research was supported by the MSIT (Ministry of Science and ICT), Korea, under the ITRC (Information Technology Research Center) support program (IITP-2023-2021-0-01816) supervised by the IITP (Institute for Information and Communications Technology Planning and Evaluation).

Data Availability Statement: Not applicable.

Conflicts of Interest: The authors declare no conflict of interest.

References

1. Choi, K.H.; Yang, E.S. A study on the trend of healthcare device technology by biometric signal. *J. Korea Entertain. Ind. Assoc.* **2020**, *14*, 165–176. [CrossRef]
2. Ferreira, J.J.; Fernandes, C.I.; Rammal, H.G.; Veiga, P.M. Wearable technology and consumer interaction: A systematic review and research agenda. *Comput. Hum. Behav.* **2021**, *118*, 106710. [CrossRef]
3. Mahloko, L.; Adebesin, F. A systematic literature review of the factors that influence the accuracy of consumer wearable health device data. In Proceedings of the e-Business, e-Services and e-Society, Skukuza, South Africa, 6–8 April 2020; pp. 96–107.
4. Singh, B.; Zopf, E.M.; Howden, E.J. Effect and feasibility of wearable physical activity trackers and pedometers for increasing physical activity and improving health outcomes in cancer survivors: A systematic review and meta-analysis. *J. Sport Health Sci.* **2022**, *11*, 184–193. [CrossRef]
5. Kim, G.; Choi, I.; Li, Q.; Kim, J. A CNN-based advertisement recommendation through real-time user face recognition. *Appl. Sci.* **2021**, *11*, 9705. [CrossRef]
6. Zhang, H. Expression-EEG based collaborative multimodal emotion recognition using deep autoencoder. *IEEE Access.* **2020**, *8*, 164130–164143. [CrossRef]
7. Gu, X.; Cai, W.; Gao, M.; Jiang, Y.; Ning, X.; Qian, P. Multi-source domain transfer discriminative dictionary learning modeling for electroencephalogram-based emotion recognition. *IEEE Trans. Comput. Soc. Syst.* **2022**, *9*, 1604–1612. [CrossRef]
8. Liu, Y.; Fu, G. Emotion recognition by deeply learned multi-channel textual and EEG features. *Future Gener. Comput. Syst.* **2021**, *119*, 1–6. [CrossRef]
9. Domínguez-Jiménez, J.A.; Campo-Landines, K.C.; Martínez-Santos, J.C.; Delahoz, E.J.; Contreras-Ortiz, S.H. A machine learning model for emotion recognition from physiological signals. *Biomed. Signal Process. Control* **2020**, *55*, 101646. [CrossRef]
10. Liu, Y.; Ding, Y.; Li, C.; Cheng, J.; Song, R.; Wan, F.; Chen, X. Multi-channel EEG-based emotion recognition via a multi-level features guided capsule network. *Comput. Biol. Med.* **2020**, *123*, 103927. [CrossRef] [PubMed]
11. Lee, J.; Yoo, S.K. Recognition of negative emotion using long short-term memory with bio-signal feature compression. *Sensors* **2020**, *20*, 573. [CrossRef] [PubMed]
12. Long, F.; Zhao, S.; Wei, X.; Ng, S.C.; Ni, X.; Chi, A.; Fang, P.; Zeng, W.; Wei, B. Positive and negative emotion classification based on multi-channel. *Front. Behav. Neurosci.* **2021**, *15*, 720451. [CrossRef] [PubMed]
13. Suhaimi, N.S.; Mountstephens, J.; Teo, J. EEG-based emotion recognition: A state-of-the-art review of current trends and opportunities. *Comput. Intell. Neurosci.* **2020**, *2020*, 8875426. [CrossRef] [PubMed]
14. Jo, C.; Jung, H. Multimodal Emotion Recognition System using Face Images and Multidimensional Emotion-based Text. *J. Korean Inst. Inf. Technol.* **2023**, *21*, 39–47.

15. Ancillon, L.; Elgendi, M.; Menon, C. Machine Learning for Anxiety Detection Using Biosignals: A Review. *Diagnostics* **2022**, *12*, 1794. [CrossRef]
16. She, W.; Lv, Z.; Taoi, J.; Niu, M. Micro-expression recognition based on multiple aggregation networks. In Proceedings of the 2020 Asia-Pacific Signal and Information Processing Association Annual Summit and Conference, Auckland, New Zealand, 7–10 December 2020.
17. Chatterjee, S. Drivers of helpfulness of online hotel reviews: A sentiment and emotion mining approach. *Int. J. Hosp. Manag.* **2020**, *85*, 102356. [CrossRef]
18. Li, J.; Hu, R.; Mukherjee, M. Discriminative Region Transfer Network for Cross-Database Micro-Expression Recognition. In Proceedings of the ICC 2022-IEEE International Conference on Communications, Seoul, Republic of Korea, 16–20 May 2022.
19. IoTKETI/Mobius: oneM2M IoT Server Platform. Available online: https://github.com/IoTKETI/Mobius (accessed on 21 April 2023).
20. Lee, S.; Kil, W.; Roh, B.H.; Kim, S.J.; Kang, J.S. Novel Architecture of OneM2M-Based Convergence Platform for Mixed Reality and IoT. *Comput. Mater. Contin.* **2022**, *71*, 51.
21. Lee, J.; Gilani, K.; Khatoon, N.; Jeong, S.; Song, J. SEIF: A Semantic-enabled IoT Service Framework for Realizing Interoperable Data and Knowledge Retrieval. *IEIE Trans. Smart Process. Comput.* **2023**, *12*, 9–22. [CrossRef]
22. Mante, S.; Vaddhiparthy, S.S.S.; Ruthwik, M.; Gangadharan, D.; Hussain, A.M.; Vattem, A. A Multi Layer Data Platform Architecture for Smart Cities using oneM2M and IUDX. In Proceedings of the 2022 IEEE 8th WF-IoT, Yokohama, Japan, 26 October–11 November 2022; pp. 1–6.
23. Peng, L.; Zheng, S.; Zhong, Q.; Chai, X.; Lin, J. A novel bagged tree ensemble regression method with multiple correlation coefficients to predict the train body vibrations using rail inspection data. *Mech. Syst. Signal Process.* **2023**, *182*, 109543. [CrossRef]
24. Šverko, Z.; Vrankić, M.; Vlahinić, S.; Rogelj, P. Complex Pearson Correlation Coefficient for EEG Connectivity Analysis. *Sensors* **2022**, *22*, 1477. [CrossRef]
25. Ning, Z.; Wang, B.; Li, S.; Jia, X.; Xie, S.; Zheng, J. Pipeline risk factors analysis using the Pearson correlation coefficient method and the random forest importance factor method. In Proceedings of the 2023 8th International Conference on Smart and Sustainable Technologies (SpliTech), Split and Bol (Island of Brac), Croatia, 20–23 June 2023; pp. 1–5
26. Otchere, D.A.; Ganat, T.O.A.; Gholami, R.; Ridha, S. Application of supervised machine learning paradigms in the prediction of petroleum reservoir properties: Comparative analysis of ANN and SVM models. *J. Pet. Sci. Eng.* **2021**, 200, 108182. [CrossRef]
27. Choi, J.; Im, S. Leak Detection and Classification of Water Pipeline based on SVM using Leakage Noise Magnitude Spectrum. *J. Inst. Electron. Inf. Eng.* **2023**, *60*, 6–14.
28. Mohammadi, M.; Rashid, T.A.; Karim, S.H.T.; Aldalwie, A.H.M.; Tho, Q.T.; Bidaki, M.; Hosseinzadeh, M. A comprehensive survey and taxonomy of the SVM-based intrusion detection systems. *J. Netw. Comput. Appl.* **2021**, *178*, 102983. [CrossRef]
29. Jebli, I.; Belouadha, F.Z.; Kabbaj, M.I.; Tilioua, A. Prediction of solar energy guided by pearson correlation using machine learning. *Energy* **2021**, *224*, 120109. [CrossRef]
30. Schaefer, A.; Nils, F.; Sanchez, X.; Philippot, P. Assessing the effectiveness of a large database of emotion-eliciting films: A new tool for emotion researchers. *Cogn. Emot.* **2010**, *24*, 1153–1172. [CrossRef]
31. Liu, Y.J.; Yu, M.; Zhao, G.; Song, J.; Ge, Y.; Shi, Y. Real-time movie-induced discrete emotion recognition from EEG signals. *IEEE Trans. Affect. Comput.* **2017**, *9*, 550–562. [CrossRef]
32. Ihmig, F.R.; Neurohr-Parakenings, F.; Schäfer, S.K.; Lass-Hennemann, J.; Michael, T. On-line anxiety level detection from biosignals: Machine learning based on a randomized controlled trial with spider-fearful individuals. *PLoS ONE* **2020**, *15*, e0231517. [CrossRef]
33. Al-Jumaily, A.A.; Matin, N.; Hoshyar, A.N. Machine learning based biosignals mental stress detection. In Proceedings of the Soft Computing in Data Science: 6th International Conference, SCDS 2021, Virtual Event, 2–3 November 2021; pp. 28–41.
34. Mekruksavanich, S.; Hnoohom, N.; Jitpattanakul, A. A Deep Residual-based Model on Multi-Branch Aggregation for Stress and Emotion Recognition through Biosignals. In Proceedings of the 2022 19th International Conference on Electrical Engineering/Electronics, Computer, Telecommunications and Information Technology (ECTI-CON), Huahin, Thailand, 24–27 May 2022; pp. 1–4.
35. Xie, S.; Girshick, R.; Dollár, P.; Tu, Z.; He, K. Aggregated residual transformations for deep neural networks. In Proceedings of the IEEE Conference on Computer Vision and Pattern Recognition (CVPR), Honolulu, HI, USA, 21–26 July 2017; pp. 1492–1500.